TANTALUM-NIOBIUM INTERNATIONAL STUDY CENTER

BULLETIN N° 71 SEPTEMBER 1992 THIRD QUARTER ISSN 1019-2026

T.I.C. activities

PHUKET, THAILAND IN NOVEMBER 1992

The Thirty-third General Assembly of the Tantalum-Niobium International Study Center will take place on November 17th 1992 as part of a meeting to be held in Phuket, Thailand, at the Meridien Hotel.

The registration desk will be open from 10a.m. to 5p.m. on Monday November 16th 1992, and all meeting participants and those accompanying them are invited to cocktails and a buffet supper party on that evening.

On Tuesday November 17th, when the formal business of the association has been carried out by the General Assembly, the rest of the day will be taken up with a technical programme which will cover industry and market reviews as well as scientific topics ranging from raw material production to the latest technology : titles of the presentations expected are listed below.

T.I.C. members Thailand Smelting and Refining, Thai Tantalum and S.A. Minerals Ltd. Partnership will kindly host a reception and dinner on Tuesday evening.

A plant tour on November 18th will visit a tin dredge, the ore-dressing plant of S.A. Minerals, and the Thaisarco tin smelter. An additional field trip offered as an option on November 19th will visit the new facility of Thai Tantalum at Mab Ta Phud.

Invitations have been sent to member companies of the T.I.C.: delegates of companies which are not members may attend the technical sessions and social events as guests, and anyone interested in participating should contact the T.I.C. at 40 rue Washington, 1050 Brussels, Belgium, without delay.

TECHNICAL PROGRAMME

The niobium market and the effect of recent technological developments
by Dr Harry Stuart and Dr Geoffrey Tither, Niobium Products Company Inc.

New technology of tantalum materials, including ultra-fine powders
by Mr Yasushi Ishimaru, Plant Manager, Vacuum Metallurgical Company

Methods for analysis of high purity niobium and tantalum
by Professor Viliam Krivan, Sektion Analytik und Höchstreinigung, Universität Ulm

The Tantalum Market in China
by Mr Nio Ming Liang, Vice Director, accompanied by Mr Zhang Jiu Ying, Ning Xia Non Ferrous Metal Smelting

New developments in the field of niobium alloys and compounds
by Dr J. Eckert, head of research in the tantalum business group, H.C. Starck

Expansion at Greenbushes tantalum mine
by Mr Malcolm Hillbeck, General Manager Operations, Gwalia Consolidated Ltd.

The nature of niobium-tantalum occurrences in Thailand
by Mr Sangat Piyasin, Geologist, Special Advisor to Thaisarco

Energy consumption in the extractive metallurgy of tantalum and niobium
by P. Paschen and G. Mori, Institut für Technologie und Hüttenkunde der Nichteisenmetalle, Montanuniversität Leoben, presented by Professor Peter Paschen

Use of tantalum and niobium in single crystal growing - lithium tantalates and lithium niobates
by Mr Shunichi Yamamoto, General Manager, Crystals Division, Electronic Materials Sector, Mitsui Mining and Smelting

Tantalum supply and demand, a statistical review
by Mr David E. Maguire, Kemet Electronics, and Mr Rod Tolley, Technical Adviser to the Tantalum-Niobium International Study Center

The outlook for tantalum, a worldwide survey
led by Dr George Korinek, NRC Inc.

VIENNA, AUSTRIA, OCTOBER 1993

The Thirty-fourth General Assembly will take place in Vienna as part of a meeting to be held from October 3rd to 5th 1993 which will include a plant tour of Treibacher Chemische Werke.

President's letter

A large market and continuous innovation are required to keep industry growing. In Europe, the EC has been unified in spite of many difficulties and in North America the USA, Canada and Mexico have realized the free trade zone concept. Such a trend may divide the world economy into separate trade blocks.

It is symbolic, I believe, that we are to have the T.I.C. meeting at Phuket in Thailand, far from Europe and also from America. The tantalum and niobium industry will not be able to grow without free trade.

Now we are facing the winter season again as we did in the early 1980's, after a rapid change in tantalum price. At that time, we could enable the tantalum industry to recover through innovation such as high CV powder and co-operation among the T.I.C. members. We need this effort again now; we should exchange information for marketing and technical innovation in order to expand the tantalum and niobium market.

It will be very important for each of the T.I.C. members to have face-to-face discussions on the future of the tantalum and niobium industry in the coming meeting at Phuket.

I am looking forward to seeing you all there.

Yoichiro Takekuro
President

T.I.C. statistics

TANTALUM

PRIMARY PRODUCTION

(quoted in lb Ta_2O_5 contained)

	2nd quarter 1992
Tin slag (2% Ta_2O_5 and over)	111499
Tantalite (all grades), other	234168
Total	345667

Note: 14 companies were asked to report, 13 replied. The companies which reported included the following, whose reports are essential before the data may be released:

Datuk Keramat Smelting, Greenbushes, Malaysia Smelting, Mamoré Mineraçao e Metalurgia, Metallurg group, Pan West Tantalum (Wodgina Mine production), Tantalum Mining Corporation of Canada, Thailand Smelting and Refining

QUARTERLY PRODUCTION ESTIMATES

(quoted in lb Ta_2O_5 contained)

LMB quotation:	*US$30*	*US$40*	*US$50*
3rd quarter 1992	309400	398600	414000
4th quarter 1992	369400	458600	474000
1st quarter 1993	377400	466600	482000
2nd quarter 1993	377400	466600	482000
3rd quarter 1993	377400	466600	482000

Note:

The quarterly production estimates are based on information available, and do not necessarily reflect total world production.

PROCESSORS' RECEIPTS

(quoted in lb Ta contained)

	2nd quarter 1992
Primary raw materials (e.g. tantalite, columbite, struverite, tin slag, synthetic concentrates)	236210
Secondary materials (e.g. Ta_2O_5, K_2TaF_7, scrap)	77760
Total	313970

Note: 17 companies were asked to report, 16 replied.

PROCESSORS'SHIPMENTS

(quoted in lb Ta contained)

Product category	*2nd quarter 1992*
Ta_2O_5, K_2TaF_7 and carbides	132230
Powder/anodes	227959
Mill products	98439
Ingot, unworked metal, other, scrap, alloy additive	58238
Total	516866

equivalent to 697770 lb Ta_2O_5.

Notes:

In accordance with the rules of confidentiality, categories have been combined as shown.

17 companies were asked to report, 16 replied in April, 17 in May and June. For both receipts and shipments by processors, reports by the following companies are essential before the data may be released:

Cabot Performance Materials, W.C. Heraeus, Kennametal, Metallurg Group, Mitsui Mining and Smelting, NRC Inc., Showa Cabot Supermetals, Hermann C. Starck Berlin, Thai Tantalum, Treibacher Chemische Werke, Vacuum Metallurgical Company, V Tech

NIOBIUM

PRIMARY PRODUCTION

(quoted in lb Nb_2O_5 contained)

	2nd quarter 1992
Concentrates: columbite, pyrochlore	8584268
Occurring with tantalum: tin slag (over 2% Ta_2O_5), tantalite, other	167627
Total	8751895

Note:

16 companies were asked to report, 14 replied. The companies which reported included the following, whose reports are essential before the data may be released: Cambior, Mineraçao Catalao de Goiás, Niobium Products Co. (CBMM)

PROCESSORS' SHIPMENTS

(quoted in lb Nb contained)

	2nd quarter 1992
Compounds and alloy additive: chemical and unwrought forms (e.g. $NbCl_5$, Nb_2O_5, NiNb, FeNb [excluding HSLA grades])	903172
Wrought niobium and its alloys in the form of mill products, powder, ingot and scrap	
(i) Pure niobium	28999
(ii) Niobium alloys (such as NbZr, NbTi and NbCu)	71662
HSLA grade FeNb	8968236
Total	9972069

Note:

18 companies were asked to report, 17 replied. Reports by the following companies are essential before the data may be released: Cabot Performance Materials, W.C. Heraeus, Kennametal, Metallurg Group, Mitsui Mining and Smelting, Niobium Products Co. (CBMM), NRC Inc., Hermann C. Starck Berlin, Teledyne Wah Chang Albany, Thai Tantalum, Treibacher Chemische Werke, Vacuum Metallurgical Company

Capacitor statistics

TANTALUM CAPACITORS IN THE U.S.

U.S. CONSUMPTION OF TANTALUM CAPACITORS

(thousands of units)

	1st quarter 1992
Metal-cased (incl. wets & foil	
Dipped (radial)	N/A
Chips	
Other (molded axial & radial)	
Total U.S. consumption	
Add U.S. production for export (all types)	
Total worldwide U.S. sales	

(Data from EIA)

EUROPEAN TANTALUM CAPACITOR SHIPMENT

(thousands of units)

1st quarter 1992	N/A

(Data from ECTSP)

JAPANESE TANTALUM CAPACITOR PRODUCTION AND EXPORTS

(thousands of units)

1st quarter 1992	
Production	1 088 061
of which exports	273 304

(Data from ECTSP)

PM '92

This year's world powder metallurgy congress was held in the San Francisco Marriott Hotel from June 21st to 26th, and the T.I.C. took a booth in the attached exhibition which ran from June 22nd to 25th. The organisation of the congress by the American powder metallurgy organisations (MPIF and APMI) was most impressive; the exhibition opened on time and in good order on the 22nd (although it would have been hard to believe it possible on the previous two days as all the machinery on display was being unpacked!), and the 300 or so congress papers were presented by topic such that up to eleven programmes were on offer at one time — and all this within the confines of the hotel basement.

I had prepared a brochure on our two metals and a copy of this, together with copies of our last two Bulletins, were given to our visitors. They proved to be of very varied backgrounds and nationalities, including large groups from the Far East (Japan, Korea and China) and from Russia. As a result, the circulation list of our quarterly Bulletin has expanded again, and several people have learnt the difference between titanium and tantalum (the niobium-titanium alloys used for superconductors led to at least some of this confusion).

I was particularly pleased to meet two men who were involved in different ways in the history of the production of tantalum as a commercial metal. The first was Mr E.R. Andreotti who worked for the Tantalum Defense Corporation (a. U.S. Government organisation) in the 1940's. He was engaged in making tantalum foil cans for the early capacitors, and sheet and wire which were used for prostheses for medical use (small clips to hold detached retinas was one application he described to me). We are very grateful to him for letting us have some of his early metal production for our archives/museum. The other was Mr M.L. McLellan who was a member of the Union Carbide team setting up the tin smelter in Phuket, Thailand in the early 1960's. They had no particular interest in the tin that would be produced: they were after the tantalum in the slags. His anecdotes of that time were of particular interest to me — I was then managing one of the two tin smelters in Malaysia which were due to lose a large part of their feed because Union Carbide, not unexpectedly, got an export embargo on tin concentrates from the Thai government as part of the deal.

The quieter periods at the exhibition were relieved by a neighbouring exhibitor who pulled in the customers for brass by running a golf putting green, and by the adhesives and bonding-agent maker across the aisle whose wall-mounted exhibits fell to the floor each night.

None of the papers presented to the congress specifically concerned tantalum or its alloys, although I was interested to learn that it is frequently used for the container in the procedure known as Hot Isostatic Pressing (HIP) because of its strength at high temperatures.

There were four descriptions of work dedicated to niobium alloys, two in presented papers and two in the form of posters* (whose authors were available each morning for discussion of their work). The first paper was from staff of Mitsubishi Materials Corporation and described their use of plasma melting in the atomisation of niobium-aluminium alloys (in particular the compound Nb_3Al, which has potential as a structural material for very high temperature applications: it melts at 1960degC). The high solidification rate when using the technique indicated its potential: a well presented paper.

The other topic in the open sessions was the production by injection moulding of two niobium superalloys, C-129-Y (niobium –12% hafnium –9% tungsten) and C-3009 (niobium –30% hafnium –9% tungsten). The constituent powders were pre-alloyed by milling, moulded to shape with a wax-polymer binder, debound and then sintered at temperatures up to 2350degC. The process shows considerable potential.

The first of the two poster entries on niobium concerned making aluminium niobide (Al_3Nb — an alloy of possible use in aerospace referred to in a recent patent — see Bulletin No69), and aluminium niobide/niobium carbide composites of high hardness by mechanical alloying (milling at elevated temperature). This interesting article was prepared by Professor Takahashi (who visited our booth) and his colleagues from the Hyogo Prefectural Institute of Industrial Research.

Finally, there was an article on the sintering of high-speed steels containing niobium presented by staff from two Brazilian research institutes, IPEN and EPUSP. Once again mechanical alloying was used (it is clearly an important advance in powder metallurgy) to produce alternative compositions in which niobium replaces the frequently used vanadium. The new technique produces an alloy in which the niobium carbide is homogeneously distributed: conventional powder metallurgy compaction gives much coarser grain size, greater porosity and lower sinterability.

Rod Tolley
Technical Adviser

* "technical notes" would be the equivalent in professional journals.

[In the next two or three Bulletins we plan to include news of the latest products and of plant modifications from those of our members which are engaged in processing tantalum and niobium. In this issue we have articles by Teledyne Wah Chang Albany and Cabot Corporation, Boyertown.
Editor]

Heat pipes for high-temperature applications

Over the past five years, Teledyne Wah Chang Albany has worked with Boeing, General Electric and General Dynamics to develop high-temperature niobium alloy heat pipes. These heat pipes resist extreme environments such as those encountered in hypervelocity aircraft (up to twenty times the speed of sound), liquid metal cooled nuclear reactors, and laser devices.

The unique ability to "superconduct" heat down the full length of the pipe enables heat pipes to resist temperatures as high as 2800-5500°F. The applied heat is spread over a large area of pipe allowing the portion of pipe which is not being heated to act as a highly efficient radiator to lower the overall temperature of the heat pipe. In fact, they are such efficient conductors of heat that when only one end of a heat pipe is heated by a torch, the entire heat pipe reaches the same temperature. To achieve such unusual heat-transfer properties, heat pipes are manufactured so that all of the interior surfaces of the pipe are covered with a porous metal wick, which acts like a sponge to absorb the heat-transfer fluid. In this example, the heat-transfer fluid is sodium or lithium. The fluid absorbs heat by vaporising at the heat

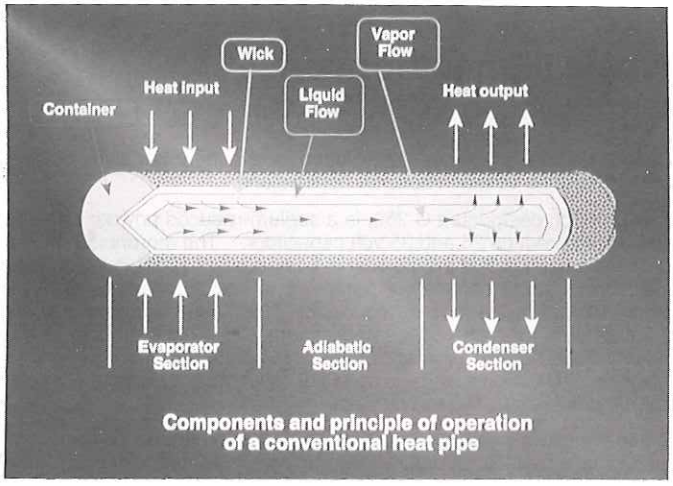

Fig. 1: Components and principle of operation of a conventional heat pipe

source and releases heat by condensing on the wick structure some distance away. Liquid metal, which condenses on to the wick, is drawn back to the heat source by capillary force thus forming a continuous cooling loop without any associated pumps, valves or other moving parts.

Work completed at TWCA has focused on developing the powder metallurgy processing methods necessary to produce very intricate niobium alloy wick structures capable of withstanding heat fluxes of 1000 to 2000watts/cm^2. Some of the prototype heat pipe parts made at TWCA include aircraft wing leading edges and nose cones for potential use on the National Aerospace Plane (NASP). The temperatures expected on the NASP missions will be much higher than those which the space shuttle tiles can withstand. Other potential applications for niobium alloy heat pipes include turbine engine and rocket motor parts.

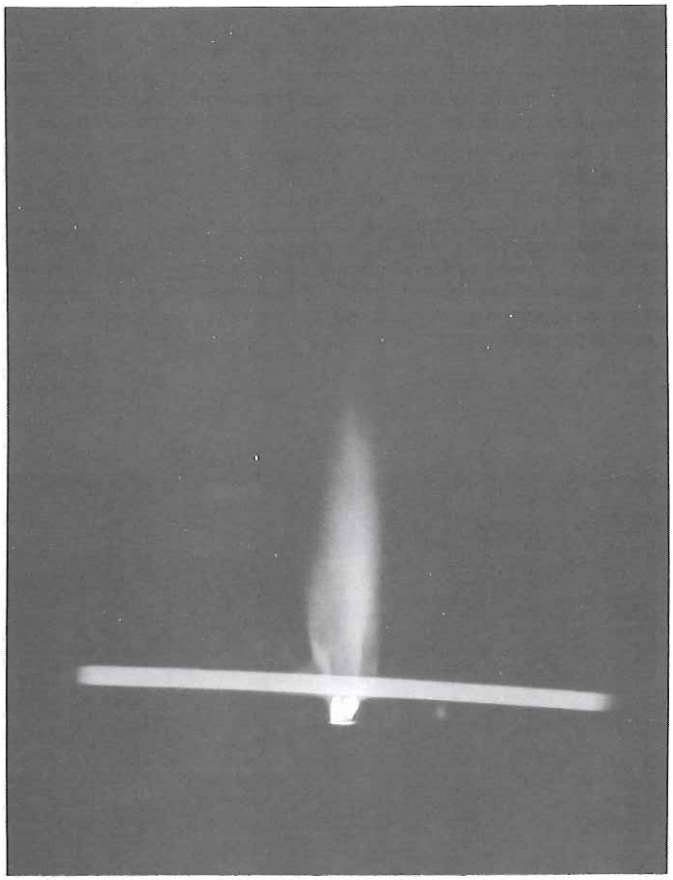

Figure 2: A C-103 alloy (Nb-10Hf-1Ti) heat pipe is heated directly in the 2800°C flame of an oxygen/mapp gas torch. To protect the surface of the C-103 from oxidation at high temperature, a protective silicide coating has been fused to the exterior surface. The pictured heat pipe measures approximately 30 cm long by 1 cm cross-section. The inside of this pipe is lined with porous niobium alloy approximately 0.6 mm thick. Lithium is the working fluid. Even though this heat pipe weighs less than 90 gm, it can withstand 2000 watts of heat input at a localised heat flux of over 1000 watts/cm^2

A new high performance tantalum powder, C-250

Cabot Corporation has recently introduced a new tantalum powder product for high voltage capacitor applications.

This product, designated C-250, is a sodium-reduced powder that can be used to produce 25 and 35 volt capacitors. The morphology of the C-250 is unique in that this powder is composed of 100% flake, with dimensions that are nominally 0.5 microns in thickness and 5 to 15 microns across the surface of the flake. This flake morphology offers the capability for high voltage applications due to the strength of the flake-to-flake bonds in the agglomerate structure and the thickness of the flake. The high surface area of flakes leads to a high capacitance after anodization to 100 to 150 volts.

C-250 tantalum powder is composed of agglomerates of flakes arranged in a box-like structure that is maintained during the pressing and sintering process commonly used to produce anodes. Pressed densities of 4.5 to 6.0g/cc can be used to achieve a high strength anode body with high porosity. This structure provides an advantage during the impregnation process where manganous (manganese II) nitrate solution is required to diffuse uniformly throughout the pore structure of the anode, followed by decomposition to manganese dioxide, forming the counter electrode.

The high porosity of the C-250 in a sintered anode is shown in the scanning electron microscope photographs in Figures 1 (30 x) and 2 (3000 x). The anode in the SEM's was sintered at temperature/time parameters that were chosen to produce an anode having a capacitance of 17000 micro-farad volts/g (CV/g).

Figure 1

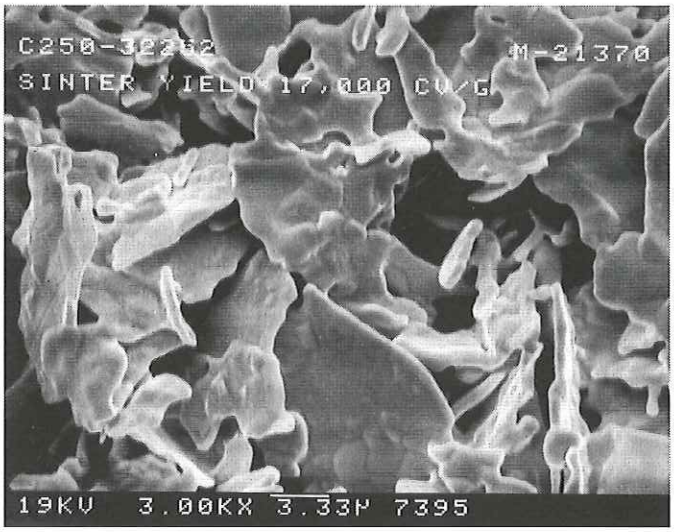

Figure 2

C-250 powder has been designed to perform at 16000 to 18000 CV/g in 35 volt capacitors and 18000 to 20000 CV/g in 25 volt capacitors. A graphical presentation of the electrical performance of this product is shown in Figures 3 and 4 where C-250 powder is compared to other commercially available Cabot powders designed for similar application areas.

The data in both graphs were obtained from co-sintered anodes.

The data in Figure 3 show the wet DCLeakage and capacitance response of C-110HP, C-310HP, C-200, C-111HP and C-250 at a formation of 150 volts. The DCLeakage response of the C-250 powder clearly shows an improvement in the capacitance potential at an equivalent DCLeakage level compared to the other Cabot tantalum powder products.

Figure 4 shows these same powders, except for C-111, at a formation voltage of 200 volts. The wet DCLeakage response of the C-250 at a 200 volt formation indicates the potential for utilization of this powder in small 50 volt capacitors.

The chemistry of tantalum powder for use in capacitor applications is very important. Oxygen levels in tantalum powder, for example, have a marked influence on the DCLeakage performance during wet testing and in the finished capacitors. The oxygen content of C-250 is controlled to a typical level of 1800 ppm, which allows the tantalum to be

subjected to multiple thermal cycles without exceeding the critical oxygen tevel in the sintered anode that will lead to excessive DCLeakage failures.

C-250 tantalum powder offers the potential for high capacitance in high voltage capacitors that are state-of-the-art in today's marketplace. This would expand the range of applications in high voltage capacitor designs for sodium reduced powders.

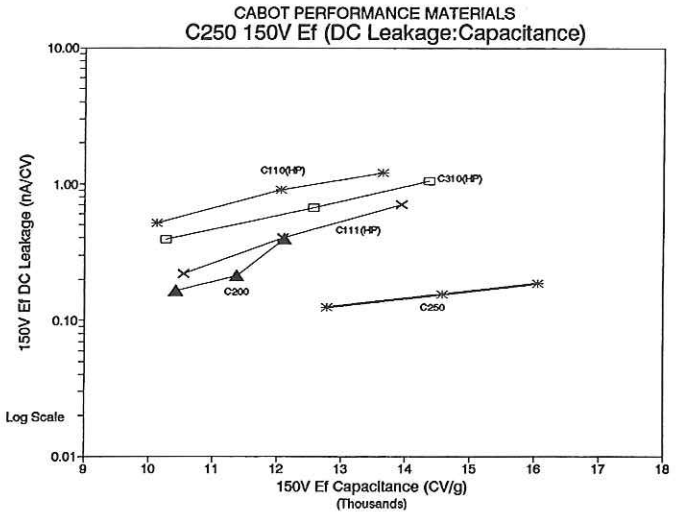

Figure 3

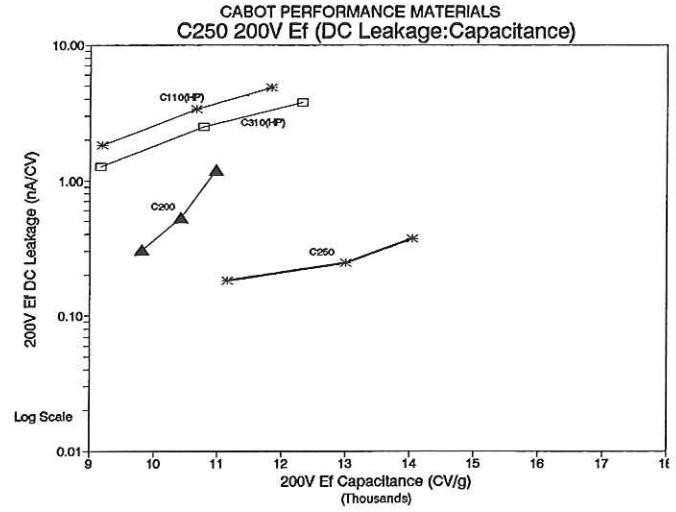

Figure 4

Refractory metals requirements for high-explosive ordnance

This paper was presented by Dr Joseph Carleone, Aerojet Electronic Systems Division, at the T.I.C. meeting held in Philadelphia in October 1991.

1. INTRODUCTION

The need for smaller, lighter, more efficient munitions has driven researchers to look at applying new materials and processes to ordnance items. Exploration of refractory metals may afford an approach to satisfy this growing need for more efficient munitions. Tungsten (W) and tantalum (Ta) are attractive alternatives to copper because of their density. Density, however, is not the only property of interest. For example, material sound speed is extremely important in controlling the tip speed of shaped-charge jets. Therefore, molybdenum (Mo) may be desirable in certain applications because of its high sound speed. Flow stress, ductility and fracture characteristics, which are highly dependent upon the manufacturing process, also determine the performance capability of these materials.

One objective of this paper is to review the material properties that are most important in controlling the performance of shaped-charge liners and explosively formed penetrators and to examine the properties of refractory metals. Another objective is to emphasize that the "dynamic" material properties must be evaluated to assess the applicability of a new material for ordnance applications. A simple comparison of typical quasi-static or handbook values will not reveal the performance of a new material in high strain-rate applications such as a shaped charge or an explosively formed projectile (EFP) charge.

To understand more fully the conditions that liner materials experience in ordnance applications, we first briefly review the mechanics of high-explosive warheads and show the extreme pressures, temperatures, strains, and strain rates that a shaped-charge or EFP liner must undergo. With this background, we group the properties into three convenient categories, (1) fundamental properties, (2) shock properties, and (3) process dependent properties. While these are not clearly mutually exclusive categories, since most of the properties are process dependent, these groupings will facilitate the discussion of high-explosive ordnance applications.

Fundamental properties are defined as density, sound speed and crystal structure. Shock properties contain the material high pressure equation-of-state and related characteristics. The third category contains those metallurgical and mechanical properties that are highly dependent on the way the materials were processed. These are grain size, constitutive properties (such as flow stress as a function of strain, strain rate and temperature), texture, and ductility or failure characteristics.

Once a material is selected for a warhead application not much can be done to improve the fundamental or shock properties, but extensive tailoring of the material to enhance performance can be achieved through proper mechanical processing. It is therefore extremely important to develop techniques which measure the appropriate dynamic properties before a material can be adequately evaluated for use in a high-explosive ordnance item.

Section 2 provides a brief review of high-explosive warheads and establishes the typical environment that warhead metallic liners experience. Section 3 compares material characteristics of copper to the three refractory metals, W, Ta, and Mo. Typical values are given and an overall discussion of how they may impact the performance of these items. Finally, a summary and conclusions are presented in Section 4.

2. ENVIRONMENT EXPERIENCED BY METAL LINERS IN HIGH-EXPLOSIVE ORDNANCE

In this section we will discuss the mechanisms by which shaped-charge jets and explosively formed projectiles (EFP) are created. The extreme pressures, temperatures, strains, and strain rates that are developed in these applications tax our understanding of materials as well as our ability to assess their ultimate performance.

2.1 Mechanics of High-Explosive Warheads.

The defeat of a target by a high explosive warhead may be described by the energy conversion process depicted in Figure 1. Some of the stored chemical energy in the high explosive is converted to kinetic energy by the warhead mechanism.

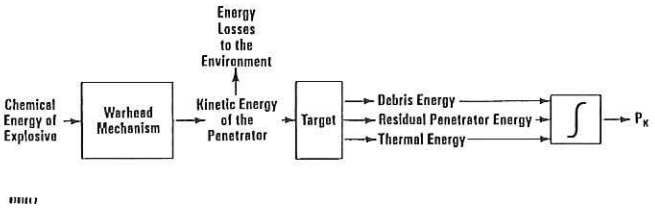

Fig. 1: The energy transfer process that occurs in the functioning of a high-explosive warhead

Depending upon the type of warhead, this kinetic energy may reside in a directed jet, a projectile of metal or in a number of metal fragments. For simplicity, we shall call the formed metal output of the warhead the penetrator. Some of the energy is also transmitted by the motion of the gases and corresponding air shock. During its flight to the target, the penetrator may lose energy to the surroundings by means of air drag, ablation, or combustion. In general, the metal penetrator interacts with the structure of the target. This interaction is a complicated process in which the target structure, and in some cases protective armor, absorbs a portion of the penetrator's kinetic energy. During the penetration process, various types of fracture mechanisms occur in both the target and the penetrator. When the outer structure and any protective armor is completely penetrated, the resultant energy delivered within the vehicle renders the damage to

"kill" the target. Somehow, we must "integrate" this delivered energy to estimate the probability of damaging the vehicle sufficiently to render it ineffective, or rather, the probability of kill, P_k.

There are five general events that occur during the functioning of a high explosive warhead. These events involve chemical, thermal and mechanical effects and are listed as follows:

- Detonation
- Metal acceleration
- Defeat mechanism formation
- Flight to the target
- Target interaction

Detonation refers to the exothermic chemical reaction that takes place in a high explosive. This reaction propagates through the unreacted explosive with such rapidity that its rate exceeds the speed of sound in the unreacted explosive. Therefore, the advancing chemical reaction zone is preceded by a shock wave, which is often called the *detonation wave*, or *detonation wavefront*. That rate of advance of this reaction zone is called the *detonation velocity*. In a high-order detonation, the detonation velocity will continue without decay through the unreacted material and is termed stable.

This reaction produces pressure pulses of very short duration with extremely high peak pressures on the order of 300-400 kbar. These pressures decay rapidly as the explosive products expand. This high pressure expansion provides the impulse to accelerate the metal casings or liners that are part of the warhead design and give rise to the blast waves and air shocks that are present when a warhead detonates.

This *metal acceleration* event essentially converts the chemical energy to kinetic energy with the metal moving at a very high final velocity. During the acceleration phase, the metal may also be formed into a particular shape to enhance the defeat of a desired target. This *defeat mechanism* formation has traditionally become the way one distinguishes between different types of warheads. These first three events: detonation, metal acceleration, and defeat mechanism formation, are depicted in Figure 2 for the examples of a shaped charge, explosively formed penetrator (EFP), and a fragmentation charge.

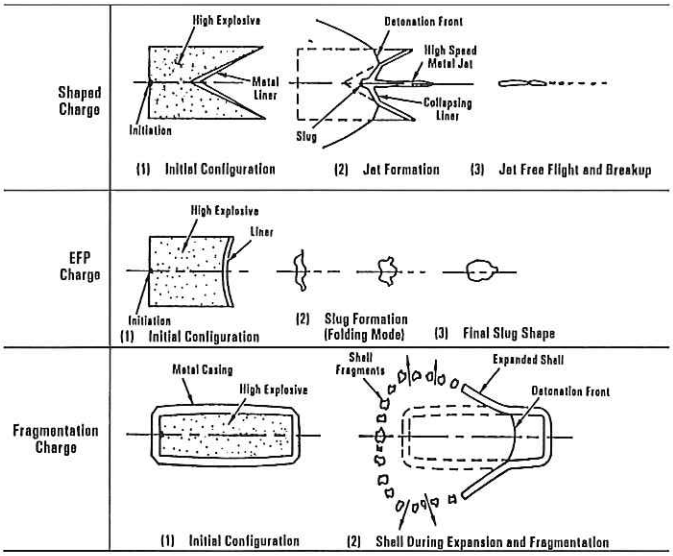

Fig. 2: General warhead mechanisms for three fundamental examples

In this paper we will focus upon explosive-metal interaction and warhead mechanism formation to determine materials requirements. Other aspects of the process of Fig. 1 is beyond the scope of this work.

2.2 Shaped Charges

This section briefly describes the mechanics of shaped charge jet formation and gives some idea of the environment that a liner experiences during this process. For more details on the shaped charge the reader is referred to the book by Walters and Zukas [1] which gives an intensive exposition of the subject and a comprehensive bibliography.

In the shaped charge, the detonation wave sweeps over the conical metal liner causing it to collapse axisymmetrically. As it collapses, liner ring elements are squeezed closer and closer to the axis. By forcing the mass radially inward, high pressures and stresses are created. The material heats up and flows plastically.

The geometry is such that a momentum exchange occurs on the axis of the charge forming a high-speed metal jet (tip speed in excess of 8 km/s) that comprises approximately 15% of the liner mass. The formation and flow of the jet seems to occur in a super-plastic taffy-like fashion. The remainder of the liner mass forms the slower-moving slug (sometimes called the carrot because of its shape). The apex portion of the liner is driven more intensely than the base portion because of the larger ratio of explosive to metal in the apex region. This causes the tip of the jet to be faster than the tail. Tip velocities can vary between 7 and 10 km/s for typical shaped charges depending on the specific design. The effective jet tail velocity is about 2 km/s. The jet therefore stretches during its flight to the target and eventually breaks into a number of segments or particles. As long as the jet segments remain aligned, the jet still penetrates deeply; however, when the shaped charge is placed at long distances from the target, the penetration is reduced because imperfections in the jet cause the segments to become misaligned. Therefore, the shaped charge is typically used in direct-hit weapons which place the warhead very close to the target.

Computer simulation of a standard conical shaped charge is shown in Figure 3. The MESA code was used to generate these simulations and selected quantities are shown at key times during jet formation to demonstrate the intense pressures, temperatures and strain rates that shaped-charge liners experience during this violent process.

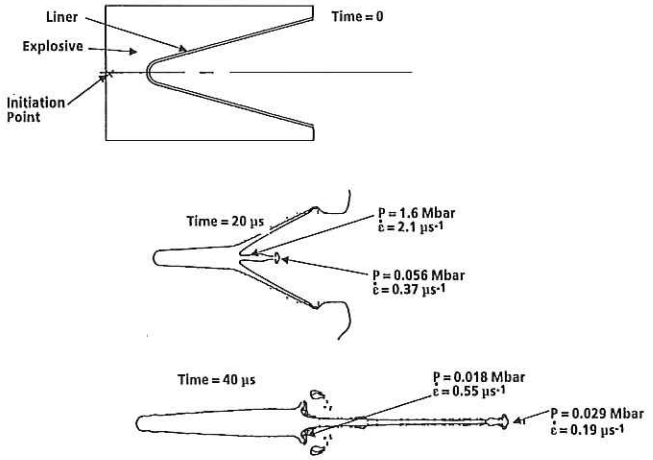

Fig. 3: Shaped-charge liner material undergoes vast swings in pressure and strain rate during jet formation

More advanced shaped-charge liner designs have evolved. By varying the liner angle along the length, greater jet stretching has been achieved. Furthermore, wall thickness variations along the length have been developed to optimize performance. This faster stretching gives greater jet length during the penetration process at short standoff and hence gives greater penetration. Details of the mechanics of penetration are beyond the scope of this paper and are covered in Ref. [1]. Suffice it to say here that for shaped charge velocities, penetration is governed primarily by total *effective* jet length and jet density.

2.3 Explosively Formed Projectiles

In contrast to a shaped charge, an explosively formed projectile (EFP, known also by the names explosively formed penetrator, self-forging fragment, Misznay-Schardin charge, P-charge, and mass focus warhead) deforms a dishshaped metal liner into a coherent projectile while accelerating it to velocities up to 3000 m/s. Nearly all of the liner mass remains in the EFP. The primary distinction between EFP and shaped charge warheads is that EFP's can be used over very long standoff distances of 150 m or more, although there are applications where the EFP is used at moderate standoffs (0.5-10 m) because of its behind-armor effectiveness when the targets are relatively thin.

In fact, the traditional shaped charge and the EFP are two extremes of the spectrum of metal-lined cavity charges. For example, as the cone angle of a shaped charge is increased beyond 150° the liner no longer splits into a jet and slug but a coherent mass or primitive EFP is formed. This has been clearly shown by Held [2]. We divide them into categories such as shaped charge, hemi charge, and EFP for convenience because the kill mechanisms in each case are formed differently and the problems associated with each are different. There are grey areas, however, that lie between the distinct categories. For example, by design, one can collapse an EFP liner hard enough to cause some jetting and elongation in which a long stretching rod is formed that eventually breaks into segments (see [3]). Such a device is neither a classical shaped charge nor an EFP. Also, a hemi charge forms a moderately fast jet without a slug. These hybrids are common and are used in various applications.

Within the family of traditional EFP warheads, however, work over the period 1975-1985 has demonstrated that virtually all practical penetrator shapes can be explosively formed by varying the contour and thickness profile of the liner in the proper way. In fact, many shapes, such as compact spheroids, long rods, hollow caps, and rods with a conical flare, have been explosively formed from thin metal discs.

Figure 4 shows a MESA simulation of a typical EFP at various stages during its formation. Note the vast swing in pressures and temperatures throughout the process. In an EFP we often attempt to absorb completely the energy that is stretching it through plastic work. When this is accomplished successfully a single-piece rod is formed. This is quite different from a shaped charge which is stretching at such a high rate that it always ultimately breaks. These design goals place different requirements on materials for EFP's as compared to shaped charges. As we will discuss in the next section, strength requirements are especially different for the two types of warhead.

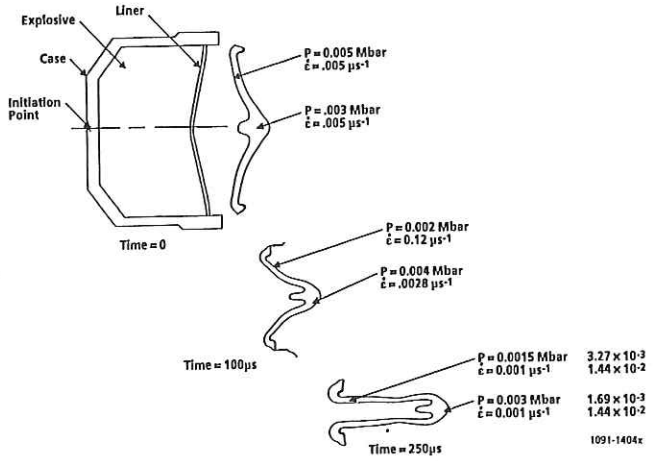

Fig. 4: EFP's undergo a rapid increase in pressure and strain rate but are designed such that the final penetrator shape no longer stretches and the material absorbs the stretching energy through plastic work

It becomes clear from the above discussion that it is highly unlikely that standard laboratory material tests are sufficient to characterize liner materials for ordnance applications. The next section addresses those properties that influence the selection of materials for both shaped-charge and EFP applications and attempts to state some of the more typical values of those properties for the three refractory metals discussed here.

3. KEY PROPERTIES OF METALS FOR HIGH-EXPLOSIVE APPLICATIONS

For convenience, we will group the properties into three categories as follows:

- Fundamental properties — density, sound speed, crystal structure
- Shock properties — shock Hugoniot, Hugoniot elastic limit, equation of state
- Process dependent properties — yield stress, flow stress, ductility, texture, grain size, fracture characteristics, ductile/brittle transition temperature.

This is not a scientifically precise grouping since one may argue that all of the properties are dependent on which process was used to produce the metal, e.g., rolling vs. forging. For practical purposes, however, this grouping provides a natural approach to discuss shaped charges and other high-explosive devices.

3.1 Fundamental Properties.

Density. The penetration of a jet, EFP, or fragment is strongly dependent upon material density. All else being equal, as density increases so does penetration depth. For shaped-charge jets at very high velocities this relationship has long been known and is embodied in the formula

$$dP = \Upsilon d\xi, \Upsilon = \sqrt{\rho_j/\rho_t} \qquad (1)$$

where dP is the increment of target penetration caused by an incremental element of jet of length $d\xi$ and ρ_j and ρ_t are the density of the jet and target respectively. As one increases the jet density to obtain greater depth, however, there is an attendant loss of hole diameter. This is due to the fact that hole volume in the target is directly related to the kinetic energy of the jet that impinges upon it. Or,

$$dV = A_H dP \sim \rho_j v_j^2 A_j d\xi \qquad (2)$$

where dV is the hole volume, A_H the hole cross-sectional area, A_j the jet cross-sectional area, and v_j, the jet velocity. We see from Eq (2) that as dP increases A_H will decrease since the impinging kinetic energy is given to be equal and we allow only density to vary for this discussion. Note that this smaller hole diameter may not allow the realization of the full penetration increase expected for shaped-charge jets. Jet waver, and perhaps tumbling of the jet segments after breakup, caused by manufacturing imprecision, become more important with a smaller hole diameter and we find the rear portions of a dense metal jet do not contribute as much to the deep penetration process as do the rear portions of jets of less dense metals.

In addition, the denser metals penetrate at a higher velocity compared to lower density materials. Therefore, it is in contact with the target during the penetration process for a shorter time. Against certain targets this may offer an advantage.

In principle, the arguments made above apply also to EFP's and fragments. Because of the lower velocity, however, the strength of target and penetrator material plays a much more important role in the process. Also, some EFP designs are hollow along the centerline or at the aft section. If this hollow is a significant percentage of the EFP cross-sectional area, then the total effect of increased material density on penetration will not be realized. In simple, but perhaps not rigorous, terms, the effective density impinging on the target is reduced by such a hollow region.

The density of three refractory metals, namely tungsten, tantalum, and molybdenum, are compared in Table I. We see a density advantage especially for W and Ta which offer approximately 40% advantage compared to copper as calculated from Eq. (1). For stretching shaped-charge jets this advantage is further compounded by allowing the rear jet elements to stretch farther prior to penetration (see [4] for more detailed arguments).

MATERIAL NAME	FUNDAMENTAL PROPERTIES: DENSITY g/cm³	FUNDAMENTAL PROPERTIES: BULK SOUND SPEED C_b (km/s)	FUNDAMENTAL PROPERTIES: CRYSTAL STRUCTURE	SHOCK PROPERTIES: HUGONIOT: $U_s = C_0 + SU_p$ C_0 (km/s)	SHOCK PROPERTIES: HUGONIOT: $U_s = C_0 + SU_p$ S	SHOCK PROPERTIES: HUGONIOT ELASTIC LIMIT (kbar)
COPPER	8.93	3.93	FCC	3.94	1.489	≈ 2
TANTALUM	16.65	3.39	BCC	3.41	1.200	≈ 8
TUNGSTEN	19.22	4.02	BCC	4.03	1.237	≈ 15
MOLYBDENUM	10.21	5.04	BCC	5.12	1.233	≈ 16

C_b ~ Calculated from Ultrasonic Measurements of C_l and C_t According to $C_b^2 = C_l^2 - \frac{4}{3} C_t^2$

U_s = Shock Velocity

U_p = Particle Velocity

Table I: Properties of copper and three refractory metals (Ref. [8])

Sound Speed. The bulk sound speed at ambient conditions may be defined in terms of the longitudinal wave speed, C_l, under a simple unistrain environment and the shear wave speed, C_t. These are defined by

$$C_l^2 = (\lambda + G)/\rho$$
$$C_t^2 = G/\rho \qquad (3)$$

where λ and G are the elastic constants of the material and can be measured directly by ultrasonic means. The bulk sound speed can then be obtained by

$$C_b^2 = C_l^2 - \frac{4}{3} C_t^2 = K/\rho \qquad (4)$$

where K is the bulk modulus of the material.

The importance of this quantity is that it controls, to some extent, the maximum tip speed of a shaped charge jet. Reference [5] showed for shaped charges that liner flow relative to the jet formation zone must remain subsonic for good, coherent jetting. Otherwise, the jet becomes radially dispersed. Using this criteria and basic jet formation theory, Carleone and Chou [6] found that, for simple conical shaped charges, the maximum jet tip speed is limited by the expression $2.41 C_b$. This approximation can be violated by more exotic designs. Since the sound speed varies with pressure, and since the formation of the jet at high pressure affects whether the liner flow is supersonic or not, such a simple expression will not govern all possibilities. The variation of sound speed with increasing pressures will be discussed in the section on shock properties.

We have not found the sound speed to be a critical property for EFP's A comparison of bulk sound speed for the three refractory metals and copper is made in Table I. From this simple comparison one may conclude that the maximum attainable jet tip speed for Ta is less than for

Cu, while that of W is equal to Cu and that of Mo is significantly greater than Cu. These facts may have some very interesting design implications which are beyond the scope of this paper.

Crystal Structure. Very little research has been published on the effect of crystal structure on the behavior of shaped-charge jets. Zernow [7] studied conical shaped charges of various materials. The experimental evidence in that report points toward the face-centered cubic (FCC) structure providing the best jet ductility with body-centered cubic (BCC) materials demonstrating the next best jet ductility. One may speculate that, with the extreme deformation that occurs in a shaped charge, the FCC structure allows for many more slip planes compared to BCC structures during this extreme deformation, and therefore yields a jet with more ductility. We have seen no evidence for a preferred crystal structure for EFP' s. Table I notes that all three refractory metals examined here are BCC structures. They do not experience any structural changes in the solid phase.

3.2 **Shock Properties**

Under explosive loading, metals experience shock waves that reverberate through them during the acceleration process. As the metallic liners collapse, intense pressures are generated and the material is often compressed significantly. To understand and model the behavior of materials under such conditions, a high-pressure equation of state is required. Such equations of state have been developed for many materials through the use of "plate-slap" experiments which measure the shock Hugoniot of the material. In these experiments, a plate of specimen material is impacted by a high-velocity flyer plate along its surface to create a one-dimensional strain field. The free surface of the plate is monitored in a unique arrangement so that the time of arrival of the shock and the motion of the surface can be measured (see [8] for details). This data allows the construction of a shock velocity U_s versus particle velocity U_p shock Hugoniot curve. Through the use of the shock equations, pressure, P, versus specific volume, V, curves can also be obtained which is the basis of an equation of state for the material. The shock Hugoniot can be represented by a straight line for many metals in the form

$$U_s = C_o + SU_P \tag{5}$$

The term C_o represents the sound speed of the material at zero pressure and can be directly compared to the bulk velocity measured using ultrasonic elastic-wave techniques. The slope S represents how sensitive the shock velocity is to the increasing particle velocity. This slope is closely associated with the repulsive forces in the lattice structure. The coefficients C_o and S are listed in Table I for copper and the refractory metals of interest. The sound speed also varies with increasing pressure. This can also be evaluated through the shock Hugoniot equation (see Ref. [8]). Figure 5 plots the variation in sound speed with local pressure in the liner material. This is very important for shaped charges since coherent jetting is related to sound speed in the formation zone which is under very high pressure. Sound speed does not appear to be a significant parameter for EFP's. Equation of state data for many materials are listed in the Los Alamos National Labs Shock Compendium [8].

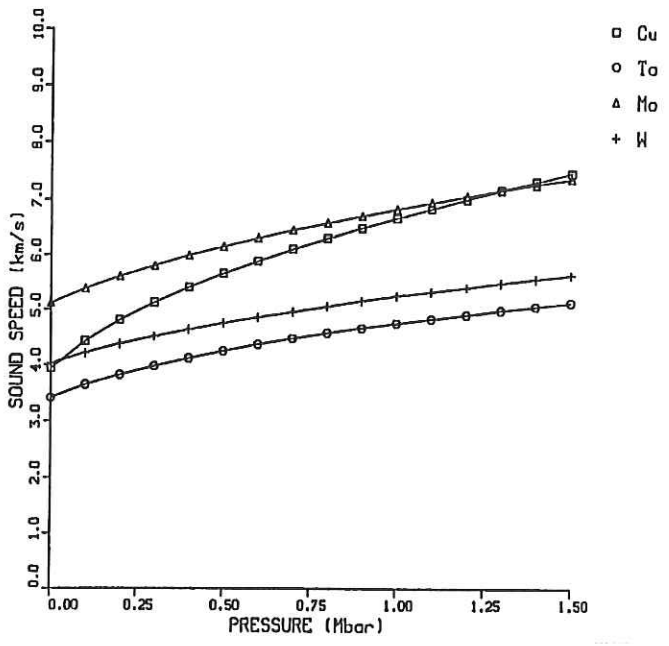

Fig. 5: Variation of sound speed with pressure

3.3 **Process-Dependent Properties**

For high-explosive applications, the material properties discussed above are usually assumed *not* to vary with the specific type of mechanical processing such as rolling, forging, deep drawing, etc. This is not totally true, however. For example, sound speed can vary somewhat if the material is anisotropic from heavy rolling in one direction. We obviously cannot address all of the possible variations with processing but will attempt here to address the more important properties for shaped charges and EFP's. In this section we focus on the behavior or response of the material to plastic flow in the high strain rate regime which is extremely sensitive to the processing of the material prior to use in the warhead configuration.

3.3.1 *Grain Size*

The grain size of the liner material can vary significantly with the method of processing the material, including the heat treatment cycle. For standard copper shaped charges grain size has been linked to jet breakup time and hence ultimate penetration capability. The trend of increased performance of copper shaped charges with liners of finer grain sizes has been well known (see [1]). For the refractory metals discussed here, such a correlation has not been drawn in the literature but has been assumed to be the case.

For EFP devices, there has been no firm correlation that grain size reduction causes increased performance. However, it is clear that strict control of the uniformity of the grain size is extremely important, as it is for shaped charges. Tantalum tends to exhibit banding of the structure as well as regions of unrecrystallized material when a very fine grain size is specified. Control of processing parameters to maintain the uniformity and size of the grains is required to obtain repeatable performance from both shaped charges and EFP's. For tantalum rolled plate as a starting liner material, grain size of ASTM 5-7 can be readily achieved and provide good performance in most applications. A slightly finer grain size can be obtained by forging liners from extruded tantalum bar. For tungsten and molybdenum, typical grain size requirements for use in shaped charges or EFP's have not yet been developed.

3.3.2 *Constitutive Properties in a Dynamic Environment*

As discussed previously, the impingement of high pressure pulses of short duration on a metallic liner subjects the material to large strains, high strain rates and increased temperatures from both shock interactions and extreme plastic work. The response of the material to this loading, exhibited by its local stress state, is extremely important to characterize in order to determine the performance of refractory metals in high-explosive devices.

In shaped charges, the jet formation can often be assumed to be purely hydrodynamic because of the intense pressures in the formation region. After the jet is formed, however, the stretching and eventual necking and segmentation is strongly dependent on the stress states and strength characteristics of the material. On the other hand, EFP liners are formed such that the strength characteristics are extremely important throughout the entire process. Thus, constitutive properties of liner materials must be measured under high rates of strain, large strains and high temperatures.

Early work on shaped charges and EFP's used a simple elastic-perfectly plastic material model. As warhead performance requirements increased, the need for a better material model became obvious.

Johnson and Cook [10] developed a constitutive model which expresses the Von Mises flow stress as a function of strain, strain-rate, and temperature and is expressed as

$$\sigma = (A + B\varepsilon^n)\,(1 + C\ln\dot{\varepsilon}^*)\,(1 - T^{*m}) \tag{6}$$

where ε is the equivalent plastic strain, $\dot{\varepsilon}^* = \dot{\varepsilon}/\dot{\varepsilon}_o$ is the dimensionless plastic strain rate for $\dot{\varepsilon}_o = 1.0\,s^{-1}$ and T is the homologous temperature which is expressed as

$$T^* = \frac{(T - T_{initial})}{(T_{melt} - T_{initial})} \tag{7}$$

The expression in the first set of brackets of Eq. (6) gives the stress as a function of strain; the second expression gives stress as a function of strain rate; and the last expression gives stress as a function of temperature. The quantities A, B, C, n, and m are the material constants. There are other constitutive models which yield reasonable results for these problems such as that presented in Reference [8]. It is not our goal to survey all available models but use this one as an example to emphasize that dynamic properties are extremely important to understand the behavior of high-explosive ordnance.

In order to determine values for the five material constants of Eq. (6), a series of laboratory tests must be conducted. The constants in the first set of brackets, A, B, and n, where A is the yield stress and B and n are strain hardening coefficients, are determined by conducting high strain rate tensile tests at room temperature and at a strain rate of

$\dot{\varepsilon}^* = 1.0$ hence eliminating rate effects and temperature effects other than adiabatic heating. The temperature effect exponent, m, is determined by repeating the high strain rate tensile test with $\dot{\varepsilon}^* = 1.0$, at elevated temperatures. Rate effects are still eliminated but strain and temperature effects are included. Finally, the strain rate coefficient, C, is determined by conducting high strain rate tests such as Hopkinson bar tests. These tests can also be conducted at room and elevated temperatures to include the effect of thermal softening. (See Nicholas [12] for a complete discussion of the Hopkinson bar test.)

After all the coefficients have been determined, a check of the basic coefficients is made by conducting Taylor tests. In a Taylor test, a cylindrical sample of the material to be used for liner fabrication is impacted upon a rigid surface at various velocities and temperatures. This test provides strains in excess of 200% and strain rates in excess of $10^5 s^{-1}$. Hydrocode simulations are conducted modeling the Taylor test, and the plastically deformed test samples are compared to the simulation. If other than minor deviations are present the constants can be varied until the two match, hence the constants are fine tuned.

Other tests can be used to determine high rate materials properties. Table II lists some of the more common tests and gives references for detailed discussion of the techniques.

Dynamic Test	Strain	Strain Rate	Pressure	Disadvantage
Hopkinson bar [12]	Moderate	Moderate	Low	Unknown friction can cause errors.
Torsion bar [13]	Large	Low	Zero	
Taylor anvil [14]	Large	Moderate	Moderate	Nonuniform loading in space and time.
Expanding ring [15]	Moderate	High	Low	Sample material may be shock hardened.

Table II: High-strain-rate test techniques

To accentuate the importance of "dynamic" properties versus static properties, we would like to discuss the following example. Tantalum sheet was fabricated by two different processes designated here as Process A and Process B. Both were processes which required the cross-rolling of pure tantalum and both had the following material properties:

- purity: 99.95%
- grain size: ASTM 6 or finer
- tensile yield stress: 35ksi maximum
- no presence of unrecrystallized areas
- no presence of banding

Process A involved melting by E-beam followed by vacuum arc remelting, cross-rolling to final thickness and finally an annealing process to recrystallize the grain structure but controlled to prohibit any substantial grain growth. On the other hand, Process B used only E-beam melting and re-melting, cross-rolling to approximately twice final thickness, an intermediate anneal, cross-rolling to final thickness, and a final anneal to recrystallize the structure without appreciable grain growth. As stated above, both Process A and Process B produced material that met the specification and had virtually identical "static" mechanical properties.

Higher strain rate tests, however, showed a significant difference in upper yield stress (and hence flow stress) at higher strain rates. This is depicted in Figure 6. We see a general increase in yield stress as strain rate increases with Process A material increasing more rapidly with strain rate. At the low strain rate (quasi static) the strength differential is negligible (approximately 2 ksi maximum). At the highest strain rate tested ($10^2 s^{-1}$), the strength differential is 10 ksi which is significant (~15%). EFP tests with the identical warhead design produced rod lengths 8-10% shorter with liners made from Process A material as compared to liners made from Process B material. The open and solid symbols denote data from two different lots of material for each process. This data may indicate more lot-to-lot variability with Process A.

For shaped-charge jets the dynamic flow stress at high temperature is extremely important because it has a strong influence on the breakup, and thus ultimate penetration, of the jet. Chou and Carleone [16] and Carleone [17] show that the breakup of the jet is directly related to $(Y/\rho)^{1/2}$ where Y is the dynamic flow stress and ρ is the jet density. Thus, to delay breakup a low value of Y is desired. Once the instability begins, however, (i.e., necks form in the jet), it would be desirable to have rate effects or work hardening take over and the material to harden in the necked region to delay the breakup even further.

The formation and final shape of EFP's are highly dependent on dynamic constitutive properties. As opposed to a classical shaped-charge jet, which will always break up at some point in time, an EFP is often designed such that the stretching kinetic energy is completely absorbed through plastic work. The end result is a single piece EFP. Some applications seek two or three pieces which is also a difficult problem in balancing strength and stretching rate. Obviously, to afford such control, the dynamic properties must be known and must be consistent for successful high-explosive ordnance performance.

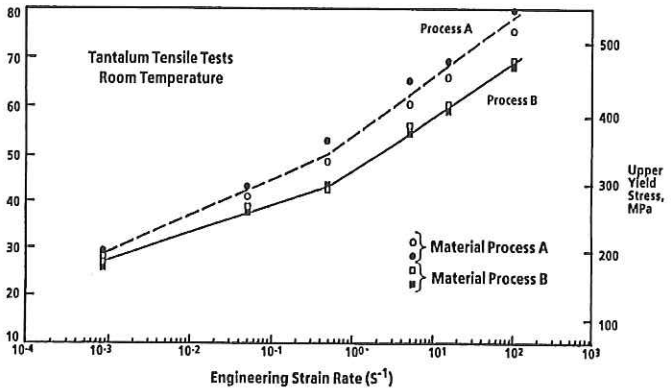

Fig. 6: Upper yield stress vs. applied strain rate

3.3.3 *Texture*

The material characteristic of crystallographic texture has been investigated by researchers on copper shaped-charge liners since the mid 70's. The work of Witt was focused on correlating metallurgical spin compensation effects with texture of the liner. Flow turning of shaped-charge liners causes the jets to spin on axis. This work showed that the flow turning affects the liner texture and correlates with the spin effect in the jet.

There has also been some correlation between shaped-charge jet ductility and texture. No correlation of texture with EFP performance has been published to date.

This area of texture requirements, for shaped-charge and EFP liners is a fruitful area for research. The texture may affect the fracture characteristics of jets and EFP's and therefore may be a factor in ultimate performance. More research needs to be conducted in this area especially for refractory metals.

3.3.4 *Fracture*

The fracture characteristics of liner materials, after they undergo the extreme conditions of jet or EFP formation, control the ultimate performance of the high-explosive device. If a shaped-charge jet experiences brittle fracture as it segments into a stream of particles, penetration is severely reduced not only because of the reduced total length but also because of the increased jet tumbling and misalignment that occurs from the nature of the fracture. Likewise EFP liners must produce rods which stretch in a ductile fashion. If brittle fracture sites occur, performance becomes highly erratic.

Because of the complexity of material deformation that occurs during formation of a shaped charge or any EFP, the total history of the deformation is important in assessing the final fracture characteristics of the material. To this end, Johnson and Cook [18] developed a cumulative damage model for materials at very high rates of strain. This model accumulates the strain history of the material deformation and is of a form similar to the Johnson and Cook strength model. Dynamic fracture tests have been defined to measure the coefficients of this fracture model and are described in [18]. Data have been published for a number of materials including copper and iron. To date no data have been presented in the literature for refractory metals. Development of such dynamic fracture data for these refractory metals will be extremely useful for warhead design.

Seaman, et al. [19] and Curran, et al. [20] have taken a different approach to material failure at high strain rate. They determine nucleation, growth and coalescence of voids, cracks or shear bands within the material that eventually lead to fracture. This approach is more physically based than other approaches and it bridges the gap between a purely continuum approach and micromechanics. The approach defines tests which can be used for both ductile and brittle materials to determine coefficients in the model. The model defined from this approach has been embedded in a few Lagrangian hydrocodes. Data have been published for a number of materials but not the refractory metals of interest. Again, it will be extremely useful to apply this approach to tantalum, tungsten and molybdenum.

It must be noted that the failure characteristics are highly sensitive to the method of material processing. One example of this is the dependence of the ductile-brittle transition temperature (DBTT) of tungsten on processing. At ambient temperatures tungsten is typically an

extremely brittle material. The heating that occurs during the functioning of ordnance items may be sufficient to cause the tungsten to become ductile. Ductility is controlled by the level of the DBTT. Two methods of processing popular for ordnance applications is warm forging and chemical vapor deposition (CVD). Lasilla and Connor [21] have determined the DBTT of tungsten for both of these processes. Figure 7 is reproduced from [21] and shows that a particular warm forging process yielded a DBTT between 150° and 200°C. The chemical vapor deposition (CVD) process they studied yielded a DBTT of 350°-400°C. One can clearly see the dependence of this important failure characteristic with process. It also must be noted that the DBTT's stated are only for those specific processes. That is, all warm forging processes and all CVD processes will not produce tungsten with the DBTT's quoted.

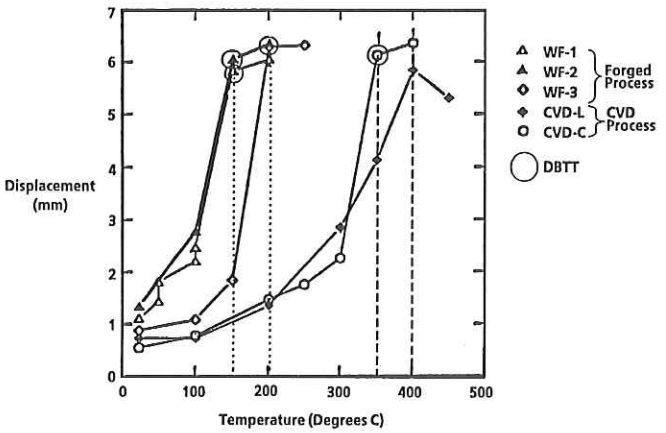

Fig. 7: Three point bend test results taken from Lasilla and Connor [21]. (Circles around the data points indicate the lowest test temperatures at which a given material did not fail. These temperatures are taken to be DBTT's as defined in this work.)

4. CONCLUSIONS

Metals used in high explosive ordnance are subjected to extremely high pressures, temperatures, strains, and strain rates. Under such conditions the mechanical behavior of these materials is quite different from their behavior at normal conditions. In the exploration of new materials for use in high-explosive devices the properties must be evaluated under these dynamic conditions through the use of unique test methods.

Refractory metals offer promise in these applications and may be an approach to increase performance or decrease the size of high-explosive ordnance. Tungsten and tantalum offer high density which directly affects penetration depth. Molybdenum offers an advantage because of its high sound speed which controls the jet tip speed and therefore the total jet length. To achieve the theoretical potential, however, the dynamic ductility and fracture characteristics of the material must be comparable to materials such as copper and aluminium in these applications.

Materials processing techniques offer an approach to tailor the material in an attempt to achieve ideal properties for high-explosive devices. The material strength and fracture characteristics of candidates control the ultimate performance in high-explosive applications. These characteristics are highly process dependent.

In summary, the success or failure of refractory metals in these applications will lie in developing the processing techniques to achieve "dynamic" properties that are optimized for high-explosive environments. It is a fruitful area for research and is likely to have significant payoff.

REFERENCES

1. Walters, W.P. and Zukas, J.A., *Fundamentals of Shaped Charges*, John Wiley & Sons, 1989.
2. Held, M., "Shaped Charge Measuring Techniques", published in notes on Fundamental Aspects of Hypervelocity Impact, Computational Mechanics Associates, 7-11 April 1986.
3. Carleone, J. and Johnson, G.R., "Multi-Slug Self-Forging Fragment Warheads", Proceedings of the First Self-Forging Fragment Conference, U.S. Army Ballistic Research Labs, 13-14 October 1982.
4. Chou, P.C. and Foster, J.C., "Theory of Penetration of Jets and Non-Linear Velocity and in Layered Targets", *Proc. 10th Int. Symp. on Ballistics*, Vol.2, San Diego, October 1987.
5. Chou, P.C., Carleone, J. and Karpp, R.R., "Criteria for Jet Formation from Impinging Shells and Plates", *J. Appl. Phys.*, Vol.47, 1976, pp.2975-2981.
6. Carleone, J. and Chou, P.C., "Maximum Jet Velocity and Comparison of Jet Breakup Models", US Army Ballistic Research Labs Report No.954, August 1955.
7. Zernow, L. and Simon, J., "High Strain Rate Plasticity of Liner Materials and Jet Behavior", US Army Ballistic Research Labs Report No.954, August 1955.
8. Kinslow, R., ed., *High Velocity Impact Phenomena*, Academic Press, New York, 1970.
9. Marsh, Stanley P., ed., *LASL Shock Hugoniot Data*, University of California Press, Univ. of Calif. Press, Berkeley and Los Angeles, CA., 1980.
10. Johnson, G.R. and Cook, W.H., "A Constitutive Model and Data for Metals Subjected to Large Strains, High Strain Rates and High Temperatures", *Proceedings of Seventh International Symposium on Ballistics*, The Hague, The Netherlands, April 1983.
11. Steinberg, D.J., Cochran, S.G. and Guinan, M.W., "A Constitutive Model for Metals Applicable at High-Strain Rate",*Journal of Applied Physics, Vol.51, No3, March 1980.*
12. Nicholas, T., "Tensile Testing of Materials at High Rates of Strain", *Experimental Mechanics*, May 1981.
13. Johnson, G.R., et al., "Response of Various Metals Subjected to Large Torsional Strains over a Large Range of Strain Rates - Part1: Ductile Metals", *Journal of Engineering Material and Technology*, ASME, Vol.105, No.1, January 1983.
14. Holmquist, T.J. and Johnson, G.R., "A Direct Method to Obtain Constitutive Model Constants from Cylinder Impact Test Results",- *Work-in-Progress at Army Symposium on Solid Mechanics*, MTL MS 86-3, West Point, New York, October 1986.
15. Warner, R.H., Karpp, R.R. and Follansbee, P.S., "The Freely Expanding Ring Test - A Test to Determine Material Strength at High Strain Rates", *Journal of Engineering Materials and Technology*, Vol.108, 1986, p.355.
16. Chou, P.C. and Carleone, J., "The Stability of Shaped Charge Jets", *J. Appl. Phys.*, Vol.48, 1977, pp.4187-4195.
17. Carleone, J., "Mechanics of Shaped Charges", Section 3, Course Notes, *Basic Principles of Hypervelocity Impact and Related Topics*, April 1987, Computational Mechanics Associates, Baltimore, MD.
18. Johnson, G.R. and Cook, W.H., "Fracture Characteristics of Three Metals Subjected to Various Strains, Strain Rates, Temperatures, and Pressures", Vol.21, 1985.
19. Seaman, L., Curran, D.R. and Shockey, D.A., "Computational Models for Ductile and Brittle Fracture", *Journal of Applied Physics*, Vol.47, November 1976.
20. Curran, D.R., Seaman, L. and Shockey, D.A., "Dynamic Failure of Solids", *Physics Reports*, Vol.147, Nos. 5 and 6, 1987.
21. Lasilla, D.H. and Connor, A., "Fracture Behavior of Warm Forged and CVD Tungsten", Lawrence Livermore National Lab, UCRL-JC-106552, 14 Feb. 1991 (A preprint).

TANTALUM-NIOBIUM INTERNATIONAL STUDY CENTER - Rue Washington 40, 1050 Brussels - Tel. (02) 649 51 58 - Telex 65080 INAC B
Fax (02) 646 05 25 PRINTED BY PUVREZ, avenue Fonsny 59, 1060 Brussels.